J|A|C|S
ARTICLES
Published on Web 11/09/2006

Development and Validation of an Integrated Computational Approach for the Modeling of cw-ESR Spectra of Free Radicals in Solution: *p*-(Methylthio)phenyl Nitronylnitroxide in Toluene as a Case Study

Vincenzo Barone,*,† Marina Brustolon,‡ Paola Cimino,†,§ Antonino Polimeno,*,‡ Mirco Zerbetto,‡ and Alfonso Zoleo‡

Contribution from the Dipartimento di Chimica and INSTM, Università di Napoli "Federico II", Complesso Universitario di Monte Sant'Angelo Via Cintia, I-80126 Napoli, Italy, and Dipartimento di Scienze Chimiche and INSTM, Università degli Studi di Padova, Via Marzolo 1, I-35131 Padova, Italy

Received August 8, 2006; E-mail: baronev@unina.it; antonino.polimeno@unipd.it

Abstract: In this work we address the interpretation, via an ab initio integrated computational approach, of continuous wave electron spin resonance (cw-ESR) spectra of *p*-(methylthio)phenyl nitronylnitroxide (MTPNN) dissolved in toluene. Our approach is based on the determination of the spin Hamiltonian, averaged with respect to fast vibrational motions, with magnetic tensor parameters (Zeeman and hyperfine tensors) characterized by quantum mechanical density functional calculations. The system is then described by a stochastic Liouville equation, with inclusion of diffusive rotational dynamics. Parametrization of diffusion rotational tensor is provided by a hydrodynamic model. Cw-ESR spectra of MTPNN are simulated for a wide range of temperatures (155−292 K) with minimal resorting to fitting procedures, proving that the combination of sensitive ESR spectroscopy and sophisticated modeling can be highly helpful in providing structural and dynamic information on molecular systems.

I. Introduction

Electron spin resonance (ESR) spectroscopy and theoretical chemistry have been entangled since the beginning of ESR. On the side of theoretical chemistry, the rich and detailed information hidden in ESR spectra has been a challenge for physicochemical interpretations and computational models. On the other hand, ESR spectroscopists have been always looking for better tools helping in interpreting the spectra. The intrinsic resolution of the ESR spectra, together with the unique role played by paramagnetic probes in providing information on their environment, makes ESR, in principle, one of the most powerful methods of investigation on the electron distribution in molecules, and on the properties of their environments. The tools needed by ESR spectroscopists are from the world of quantum mechanics calculations, as far as the parameters of the spin Hamiltonian are concerned, and from the world of molecular dynamics and statistical thermodynamics for the spectral line shapes.

The introduction of the density functional theory (DFT) was a turning point for the calculations of the spin Hamiltonian parameters.[1] Before DFT, ab initio calculations of the magnetic parameters of spin Hamiltonians were either prohibitively expensive already for medium-sized radicals[2] or less reliable than semiempirical methods. These latter were based on the approaches introduced by McConnell[3] and Stone[4] for the calculations of the hyperfine coupling and the **g** tensors, respectively. Based on semiempirical parameters taking into account separately the spin density on the SOMO and that due to spin polarization,[5] the method for the evaluation of hyperfine tensors has been an invaluable tool for understanding the correlation between the magnetic parameters of the spin Hamiltonian, the spin distribution, the conformation of radicals, the molecular properties in general. However, the reliability of the method was very restricted, as limited to predictions inside groups of similar radicals for which the same set of semiempirical parameters were sound, and the parameters to be calculated were only the SOMO spin densities.[5] Within these limits the calculated hyperfine tensors were quite reliable.

On the other hand, the agreement between calculated and experimental values for **g** tensors in general used to be much

† Università di Napoli "Federico II".
‡ Università degli Studi di Padova.
§ Permanent address: Dipartimento di Scienze Farmaceutiche, Università di Salerno, Via Ponte Don Melillo, 84084 Fisciano-Salerno, Italy.

(1) (a) Barone, V. *J. Chem. Phys.* **1994**, *101*, 6834. (b) Barone, V. *J. Chem. Phys.* **1994**, *101*, 10666. (c) Barone, V. *Theor. Chem. Acc.* **1995**, *91*, 113. (d) Barone, V. In *Advances in Density Functional Theory*, part I; Chong, D. P., Ed.; World Science Publishing Co.: Singapore, 1995; Vol. 287. (e) Improta, R.; Barone, V. *Chem. Rev.* **2004**, *104*, 1231.
(2) (a) Feller, D.; Davidson, E. R. *J. Chem. Phys.* **1988**, *88*, 5770. (b) Engels, B.; Eriksson, L. A.; Lunell, S. *Advances in Quantum Chemistry*; Academic Press: San Diego, 1996; Vol. 27, p 297. (c) Perera, S. A.; Salemi, L. M.; Bartlett, R. J. *J. Chem. Phys.* **1997**, *106*, 4061. (d) Al Derzi, A. R.; Fan, S.; Bartlett, R. J. *J. Phys. Chem. A* **2003**, *107*, 6656.
(3) (a) McConnell, H. M. *J. Phys. Chem.* **1963**, *39*, 1910. (b) McConnell, H. M. *Proc. R. A. Welch Found. Conf. Chem. Res.* **1967**, *11*, 144.
(4) (a) Stone, A. J. *Proc. R. Soc. London, Ser. A* **1963**, *271*, 424. (b) Stone, A. J. *Mol. Phys.* **1964**, *6*, 311.
(5) Adamo, C.; Barone, V.; Subra, R. *Theor. Chem. Acc.* **2000**, *104*, 207.

worse. To this end, it should be noted that the recently achieved chances of calculating reliable **g** tensor principal values by DFT on one hand,[6−9] and to measure them by high-frequency ESR on the other one, has provided a new largely unexplored source of information on molecular properties attainable by ESR analysis.

Today, the agreement between experimental and calculated parameters of the spin Hamiltonian by DFT is outstanding.[1,8,9] Both the vibrational averaging of the parameters[10] and the interactions of the probe with the environment[11,12] are taken into account, thereby providing a set of tailored parameters that can be used confidently for further calculations. It should be noted that this approach is a step forward with respect to the traditional starting point, i.e., the use of a set of experimental hyperfine and **g** tensors generally obtained for a different system, and extrapolated to the case of interest.

The other challenging experimental/theoretical match, ESR spectral profile versus molecular dynamics, has a long history too. The two limits of essentially fixed molecular orientation, as in a crystal, and of rapidly rotating probes in solutions of low viscosity (Redfield limit)[13] have been overcome by methods based on the stochastic Liouville approach, allowing the simulation of spectra in any régime of motion and in any type of orienting potential.[14] Due to the largely diffuse interest for the applications involving nitroxide spin probes in biological systems, the simulation programs allowing the combined effects of motions of different rates have been written for this type of probes, taking into account the hyperfine coupling with a single nitrogen nucleus.

ESR spectroscopy is an essential tool in material science also. In particular, the search of new materials with tailored magnetic properties has intensified in recent years. In this field the most popular stable radicals are nitronylnitroxide (NIT) free radicals. They exhibit a large variety of magnetic behavior: paramagnetism down to very low temperature, ferromagnetism, antiferromagnetism.[15] Moreover, the nitronylnitoxides have also been known as bidentate ligands for various transition and rare-earth metal ions. Ferromagnetic ground states have been observed also in these complexes.[16] For these particular magnetic properties NIT radicals are particularly appealing as molecular units for composite new materials. One of the driving forces of the present work was the demand for simulations of ESR spectra of NIT in any régime of motion, not available up to today.

In the path towards new magnetic materials, the characterization of the electronic distributions and magnetic properties of isolated radicals is of primary interest. Theoretical predictions of the spin distribution on the radicals by DFT calculations are necessary in order to understand the radical−radical interactions in bulk and composite materials. On the other hand, the spin density depends strongly on the interaction with the environment that can be very complex in a composite material.

Nowadays the improved methods in calculations of spin density distribution, **g** tensors, and other magnetic parameters on one hand and of the ESR line shapes on the other one make it possible to build a new and exciting tool that allows extraction of straightforward physicochemical information from the ESR spectra. Here, we will show that for a prototypical nitronylnitroxide radical (*p*-(methylthio)phenyl nitronylnitroxide, MTPNN)[17] in a simple environment as a toluene solution, starting simply from the structural formula of the radical and the physical parameters of the solvent, it is possible to calculate ESR spectra showing afterward an exceptionally good agreement with the experimental ones, from room temperature to a temperature very near to the glassy transition. This is done by integrating a DFT evaluation of geometry and magnetic parameters of the radical in its environment with a stochastic Liouville approach for the calculation of the spectral profile. We point out the difference between this approach and the traditional spectra simulation. As the dynamical properties of the radical depend on the diffusion tensor, that in turn depends on the minimum energy conformation of the radical, a back and forth path improving the agreement between experimental and calculated spectrum improves directly the understanding of the physicochemical properties of the system. Moreover, the conformation of the radical affects the magnetic tensors, with a further bias on the reliability of the model. A similar positive entanglement is present also between the radical/environment interaction conditioning the values of the hyperfine and **g** tensors, and the effects of the latter values on the positions and shapes of the ESR lines. The self-consistency of the method correlates all the parameters that arise from a precise model of the radical in its environment. A disagreement between the calculated and experimental spectra requires therefore a different hypothesis on the nature of the radical/environment system.

On the contrary, in spectra simulation the two steps of guessing the magnetic parameters and of simulating the spectral profile are completely disentangled. The best fit provides a number of partially uncorrelated parameters that can be varied independently, without any substantial fallout on the reliability of the whole model.

We believe, therefore, that the ESR spectral calculation method introduced here below represents a fundamental step in putting together the best up-to-date quantum mechanical (QM) calculations of spin Hamiltonian parameters and methods of

(6) (a) Neese, F. *J. Chem. Phys.* **2001**, *115*, 11080. (b) Ditchfield, R. *Mol. Phys.* **1974**, *27*, 789. (c) Cheesman, J. R.; Trucks, G. W.; Keith, T. A.; Frisch, M. J. *J. Chem. Phys.* **1998**, *104*, 5497.
(7) Malkina, O. L.; Vaara, J.; Schimmelpfenning, J. B.; Munzarova, M. L.; Malkin, V. G.; Kaupp, M. J. *J. Am. Chem. Soc.* **2000**, *122*, 9206.
(8) Kaupp, M.; Reviakine, R.; Malkina, O. L.; Arbuznikov, A.; Schimmelpfenning, G.; Malkin, V. G. *J. Comput. Chem.* **2002**, *23*, 794.
(9) Ciofini, I.; Adamo, C.; Barone, V. *J. Chem. Phys.* **2004**, *121*, 6710.
(10) (a) Barone, V.; Subra, R. *J. Chem. Phys.* **1996**, *104*, 2630. (b) Jolibois, F.; Cadet, A.; Grand, R.; Subra, R.; Barone, V.; Rega, N. *J. Am. Chem. Soc.* **1998**, *120*, 1864. (c); Barone, V.; Carbonniere, P.; Pouchan, C. *J. Chem. Phys.* **2005**, *122*, 224308.
(11) (a) Nillson, J. A.; Eriksson, L. A.; Laaksonen, A. *Mol. Phys*. **2001**, *99*, 247. (b) Nonella, M.; Mathias, G.; Tavan, P. *J. Phys. Chem. A* **2003**, *107*, 8638. (c) Asher, J. R.; Doltsinis, N. L.; Kaupp, M. J. *Magn. Reson. Chem.* **2005**, *43*, S237.
(12) (a) Pavone, M.; Benzi, C.; De Angelis, F.; Barone, V. *Chem. Phys. Lett*. **2004**, *395*, 120. (b) Pavone, M.; Cimino, P.; De Angelis, F.; Barone, V. *J. Am. Chem. Soc*. **2006**, *128*, 4338. (c) Pavone, M.; Sillampa, A.; Cimino, P.; Crescenzi, O.; Barone, V. *J. Phys. Chem. B* **2006**, *110*, 16189.
(13) Slichter, C. P. *Principles of Magnetic Resonance*; Harper & Row: New York, 1963.
(14) Moro, G.; Freed, J. H. In *Large-Scale Eigenvalue Problems*; Cullum, J., Willoughby, R., Eds.; Mathematical Studies Series, Vol. 127; Elsevier: New York, 1986. Schneider, D. J.; Freed, J. H. *Adv. Chem. Phys.* **1989**, *73*, 487.
(15) Osiecki, J. H.; Ullman, E. F. *J. Am. Chem. Soc.* **1968**, *90*, 1078.
(16) (a) Awaga, K.; Inabe, T.; Okayama, T.; Maruyama, Y. *Mol. Cryst. Liq. Cryst*. **1993**, *232*, 79. (b) Caneschi, A.; Chiesi, P.; David, L.; Ferraro, F.; Gatteschi, D.; Sessoli, R. *Inorg. Chem*. **1993**, *32*, 1445. (c) Caneschi, A.; Ferraro, F.; Gatteschi, D.; Le Lirzin, A.; Novak, M.; Rentschler, E.; Sessoli, R. *Adv. Mater*. **1995**, *7*, 476. (d) Gorini, L.; Caneschi, A.; Menichetti, S. *Synlett* **2006**, *6*, 948. (e) Caneschi, A.; David, L.; Ferraro, F.; Gatteschi, D.; Fabretti, A. C. *Inorg. Chim. Acta* **1995**, *235*, 159.
(17) Pillet, S.; Souhassou, M.; Pontillon, Y.; Caneschi, A.; Gatteschi, D.; Lecomte, C. *New J. Chem.* **2001**, *25*, 131.

simulations of spectral profile, making ESR spectroscopy a still more powerful tool in several research fields.

The paper is organized as follows. After the experimental details, in section III we recall the molecular structure of the system under investigation, we present the SLE and the computational approach employed to calculate ESR spectra. Results are presented in section IV together with some general conclusions.

II. Experimental Details

MTPNN was a kind gift from Gatteschi's group. A description of the synthesis of MTPNN can be found in refs 16 d and e. The cw-ESR sample was prepared dissolving MTPNN in toluene to a concentration of 1×10^{-4} M. About 100 μL of solution were introduced into a high-quality quartz tube. The tube was connected to a vacuum line, and oxygen in the toluene solution was fully removed by several freeze-and-thaw cycles. Eventually, the tube was sealed under vacuum. Cw-ESR spectra were recorded at the X-band frequency (about 9.7 GHz) using a Bruker ELEXSYS instrument equipped with a high-quality dielectric resonator, a cryostat Oxford CF935, and a variable-temperature unit Oxford ITC 4. Temperature was lowered in steps of 10 K from 292 K down to 155 K, and the system was stabilized at each temperature at least 1 h before the measurement. Instrumental acquisition parameters such as microwave power and amplitude modulation were carefully chosen to avoid saturation effects and spectral line shape distortion.

Microwave frequency was measured for each spectrum using a 5342A HP frequency counter, and DPPH was used as a standard for *g*-value calibration. The experimental *g*-value determination was done by taking the inflection point of the center line of the ESR spectrum.

III. Modeling and Interpretation

III.A. Molecular System. Commonly employed paramagnetic probes in ESR studies are nitroxide derivatives, which have been extensively used for characterization of structural and dynamic behavior of isotropic and ordered phases and complex molecular systems,[18−21] with particular emphasis on biological macromolecules.[21,22] They are widely employed in cw-ESR, pulsed ESR or ENDOR spectra. As probes or spin labels they are employed extensively to obtain information on structural and dynamic properties of biomolecules, micelles, and membranes.[21] In particular, measurements performed on proteins via site-directed spin labeling (SDSL) are highly informative.[22] They are well-characterized systems, both in terms of magnetic properties (**A** and **g** tensors) and dynamical properties (rotational diffusion). The development of simulation programs of their cw-ESR spectra in the presence of several relaxation processes due to motions in different dynamical ranges (see, for example, the slowly relaxing local structure model, SRLS) has led to a number of applications in liquids, liquid crystalline phases, composite materials, and biological systems.[18−21]

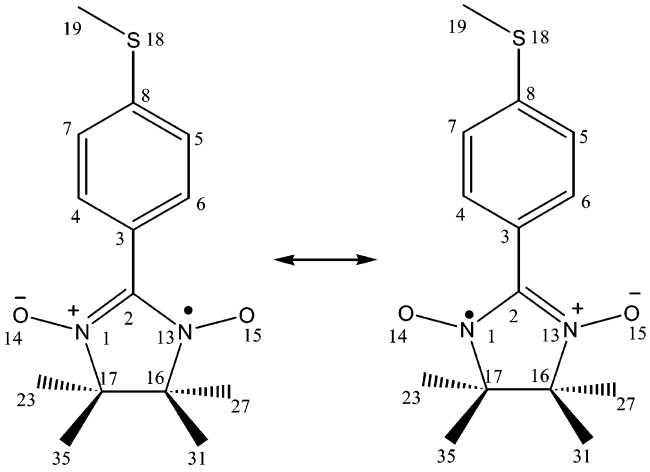

Figure 1. Structure of *p*-(methylthio)phenyl nitronylnitroxide (MTPNN).

On the other side, the employment of NIT radicals in cw-ESR esperiments is relatively recent, and it appears to be of relevance for their significant stability and variety of magnetic behavior, mostly in the context of material science. NIT free radicals are particularly appealing as molecular units for composite new materials, and ESR is the tool of election to monitor structural and dynamical characteristics. However, the presence of the coupling of the unpaired electron with two nitrogen nuclei makes this probe different from nitroxides, and specific simulation programs of ESR spectra of NIT in any régime of motion are not available up to today. They are approached in this work for the first time.

We shall consider *p*-(methylthio)phenyl nitronylnitroxide (MTPNN) as a prototype NIT radical. A schematic overview of the molecule is shown in Figure 1, which illustrates the chemical structure of the paramagnetic probe stressing the coupling of the unpaired electron with two ^{14}N. The molecule is characterized by a nitroxylnitroxide group linked to a methylthio-phenyl group.

III.B. Ab Initio Integrated Computational Approach. We present here some qualitative considerations on the foundation of an ab initio integrated computational approach (ICA) to the interpretation of cw-ESR spectra of free radicals.[23] The calculation of ESR observables can in principle be based on the complete solution of the Schrödinger equation for the system made of a paramagnetic probe + explicit solvent molecules. The system can be described by a "complete" Hamiltonian $\hat{H}(\{\mathbf{r}_i\},\{\mathbf{R}_k\},\{\mathbf{q}_\alpha\})$, which can be written in the form

$$\hat{H}(\{\mathbf{r}_i\},\{\mathbf{R}_k\},\{\mathbf{q}_\alpha\}) = \hat{H}_{\text{probe}}(\{\mathbf{r}_i\},\{\mathbf{R}_k\}) + \hat{H}_{\text{probe-solvent}}(\{\mathbf{r}_i\},\{\mathbf{R}_k\},\{\mathbf{q}_\alpha\}) + \hat{H}_{\text{solvent}}(\{\mathbf{q}_\alpha\}) \quad (1)$$

where probe and solvent terms are separated. Hamiltonian $\hat{H}(\{\mathbf{r}_i\},\{\mathbf{R}_k\},\{\mathbf{q}_\alpha\})$ contains (*i*) electronic coordinates $\{\mathbf{r}_i\}$ of the paramagnetic probe (where index *i* runs on all probe electrons), (*ii*) nuclear coordinates $\{\mathbf{R}_k\}$ (where index *k* runs on all ρ-vibrational nuclear coordinates) and (*iii*) *coordinates* $\{\mathbf{q}_\alpha\}$, in which we include all degrees of freedom of all solvent molecules, each labeled by index α. The basic object of study, to which any spectroscopic observable can be linked, is given by the density matrix $\hat{\rho}(\{\mathbf{r}_i\},\{\mathbf{R}_k\},\{\mathbf{q}_\alpha\},t)$, which in turn is

(18) Borbat, P. P.; Costa-Filho A. J.; Earle, K. A.; Moscicki, J. K.; Freed, J. H. *Science* **2001**, *291*, 266.
(19) Meirovitch, E.; Igner, D.; Igner, D.; Moro, G.; Freed, J. H. *J. Chem. Phys.* **1982**, *77*, 3915.
(20) (a) Polimeno, A.; Freed, J. H. *J. Phys. Chem.* **1995**, *99*, 10995. (b) Polimeno, A.; Freed, J. H. *Adv. Chem. Phys.* **1993**, *83*, 89.
(21) Liang, Z.; Lou, Y.; Freed, J. H.; Columbus, L.; Hubbell, W. L. *J. Phys. Chem. B* **2004**, *108*, 17649.
(22) (a) Luckhurst, G. R. In *Spin Labeling, Theory and Applications*; Berliner, L. J., Ed.; Academic Press: New York, 1976; pp 133−181. (b) Meier, P.; Blume, A.; Ohmes, E.; Neugebauer, F. A.; Kothe, G. *Biochemistry* **1982**, *21*, 526. (c) Möbius, K.; Savitsky, A.; Wegener, Ch.; Plato, M.; Fuchs, M.; Schnegg, A.; Dubinskii, A. A.; Grigor'ev, I. A.; Kühn, M.; Duché, D.; Zimmermann, H.; Steinhoff H.-J. *Magn. Reson. Chem.* **2005**, *43*, S4−S19.
(23) Barone V.; Polimeno, A. *Phys. Chem. Chem. Phys.* **2006**, *8*, 4609.

obtained from the Liouville equation

$$\frac{\partial}{\partial t}\hat{\rho}(\{\mathbf{r}_i\},\{\mathbf{R}_k\},\{\mathbf{q}_\alpha\},t) = -i[\hat{H}(\{\mathbf{r}_i\},\{\mathbf{R}_k\},\{\mathbf{q}_\alpha\}), \hat{\rho}(\{\mathbf{r}_i\},\{\mathbf{R}_k\},\{\mathbf{q}_\alpha\},t)] = -\hat{L}(\{\mathbf{r}_i\},\{\mathbf{R}_k\},\{\mathbf{q}_\alpha\})\,\hat{\rho}(\{\mathbf{r}_i\},\{\mathbf{R}_k\},\{\mathbf{q}_\alpha\},t) \quad (2)$$

Solving eq 2 in time—for instance via an ab initio molecular dynamics scheme—allows in principle the direct evaluation of $\hat{\rho}(\{\mathbf{r}_i\},\{\mathbf{R}_k\},\{\mathbf{q}_\alpha\},t)$ and hence calculation of any molecular property. However, significant approximations are possible, which are basically rooted in time-scale separation. The nuclear coordinates $\mathbf{R} \equiv \{\mathbf{R}_k\}$ can be separated into fast-probe vibrational coordinates $\mathbf{R}_{\text{fast}}$ and slow-probe coordinates, i.e., intermolecular rotation degrees of freedom and, if required, intramolecular "soft" torsional degrees of freedom, $\mathbf{R}_{\text{slow}}$, relaxing at least in a picoseconds time scale. Then the probe Hamiltonian is averaged on (*i*) femtoseconds and subpicoseconds dynamics, pertaining to the probe of electronic coordinates and (*ii*) picoseconds dynamics, pertaining to the probe of internal vibrational degrees of freedom. The averaging on the electron coordinates is the usual implicit procedure for obtaining a spin Hamiltonian from the complete Hamiltonian of the radical. In the frame of Born−Oppenheimer approximation, the averaging on the picosecond dynamics of nuclear coordinates allows introduction of the effect of the vibrational motions into the calculation of magnetic parameters, that can be very relevant in some cases.[10] In this way a probe Hamiltonian is obtained that is characterized by magnetic tensors. By taking into account only the electron Zeeman and the hyperfine interactions, for a probe with one unpaired electron and *N* nuclei we can define an averaged magnetic Hamiltonian $\hat{H}(\mathbf{R}_{\text{slow}},\{\mathbf{q}_\alpha\})$:

$$\hat{H}(\mathbf{R}_{\text{slow}},\{\mathbf{q}_\alpha\}) = \frac{\beta_e}{\hbar}\mathbf{B}_0\cdot\mathbf{g}(\mathbf{R}_{\text{slow}},\{\mathbf{q}_\alpha\})\cdot\hat{\mathbf{S}} + \gamma_e\sum_n \hat{\mathbf{I}}_n\cdot\mathbf{A}_n(\mathbf{R}_{\text{slow}},\{\mathbf{q}_\alpha\})\cdot\hat{\mathbf{S}} + \hat{H}_{\text{probe-solvent}}(\mathbf{R}_{\text{slow}},\{\mathbf{q}_\alpha\}) + \hat{H}_{\text{solvent}}(\{\mathbf{q}_\alpha\}) \quad (3)$$

The first term is the Zeeman interaction depending upon the $\mathbf{g}(\mathbf{R}_{\text{slow}},\{\mathbf{q}_\alpha\})$ tensor, external magnetic field $\mathbf{B}_0$, and electron spin momentum operator $\hat{\mathbf{S}}$; the second term is the hyperfine interaction of the *n*th nucleus and the unpaired electron, defined with respect to hyperfine tensor $\mathbf{A}_n(\mathbf{R}_{\text{slow}},\{\mathbf{q}_\alpha\})$ and nuclear spin momentum operator $\mathbf{I}_n$. Additional terms are $\hat{H}_{\text{probe-solvent}}(\mathbf{R}_{\text{slow}},\{\mathbf{q}_\alpha\})$ for accounting interactions between the probe and the medium which do not affect directly the magnetic properties (e.g., solvation energy) and $\hat{H}_{\text{solvent}}(\{\mathbf{q}_\alpha\})$ for solvent-related terms. Here, tensors $\mathbf{g}(\mathbf{R}_{\text{slow}},\{\mathbf{q}_\alpha\})$ and $\mathbf{A}_n(\mathbf{R}_{\text{slow}},\{\mathbf{q}_\alpha\})$ are diagonal in local (molecular) frames GF, A_iF; operators I_n, *S* are defined in the laboratory or inertial frame (LF). An explicit dependence is left in the magnetic tensor definition from slow-probe coordinates (e.g. geometrical dependence upon rotation), and solvent coordinates. The averaged density matrix becomes $\hat{\rho}(\mathbf{R}_{\text{slow}},\{\mathbf{q}_\alpha\},t) = \langle\hat{\rho}(\{\mathbf{r}_i\},\{\mathbf{R}_k\},\{\mathbf{q}_\alpha\},t)\rangle_{\{\mathbf{r}_i\},\mathbf{R}_{\text{fast}}}$ and the corresponding Liouville equation, in the hypothesis of no residual dynamic effect of averaging with respect to subpicoseconds processes, can be simply written as in eq 2 with $\hat{H}(\mathbf{R}_{\text{slow}},\{\mathbf{q}_\alpha\})$ instead of $\hat{H}(\{\mathbf{r}_i\},\{\mathbf{R}_k\},\{\mathbf{q}_\alpha\})$.

Finally, the dependence upon solvent or bath coordinates can be treated at a classical mechanical level, either by solving explicitly the Newtonian dynamics of the explicit set $\{\mathbf{q}_\alpha\}$ or by adopting standard statistical thermodynamics argument. This is formally equivalent to averaging the density matrix with respect to solvent variables $\hat{\rho}(\mathbf{R}_{\text{slow}},t) = \langle\hat{\rho}(\mathbf{R}_{\text{slow}},\{\mathbf{q}_\alpha\},t)\rangle_{\{\mathbf{q}_\alpha\}}$. The modified time evolution equation for $\hat{\rho}(\mathbf{R}_{\text{slow}},t)$ can efficiently be interpreted within the framework of explicit stochastic modeling according to the so-called stochastic Liouville equation (SLE) formalism, defined by the direct inclusion of motional dynamics in the form of stochastic (Fokker−Planck/diffusive) operators in the Liouvillean governing the time evolution of the system[14]

$$\frac{\partial}{\partial t}\hat{\rho}(\mathbf{R}_{\text{slow}},t) = -i[\hat{H}(\mathbf{R}_{\text{slow}}),\,\hat{\rho}(\mathbf{R}_{\text{slow}},t)] - \hat{\Gamma}\hat{\rho}(\mathbf{R}_{\text{slow}},t) = -\hat{L}(\mathbf{R}_{\text{slow}})\hat{\rho}(\mathbf{R}_{\text{slow}},t) \quad (4)$$

where the effective Hamiltonian, averaged with respect to the solvent coordinates, is

$$\hat{H}(\mathbf{R}_{\text{slow}}) = \frac{\beta_e}{\hbar}\mathbf{B}_0\cdot\mathbf{g}(\mathbf{R}_{\text{slow}})\cdot\hat{\mathbf{S}} + \gamma_e\sum_n \hat{\mathbf{I}}_n\cdot\mathbf{A}_n(\mathbf{R}_{\text{slow}})\cdot\hat{\mathbf{S}} \quad (5)$$

and $\mathbf{g}(\mathbf{R}_{\text{slow}})$, $\mathbf{A}_n(\mathbf{R}_{\text{slow}})$ are now averaged tensors with respect to solvent coordinates, while $\hat{\Gamma}$ is the stochastic (Fokker−Planck or Smoluchowski) operator modeling the dependence of the reduced density matrix on relaxing processes described by stochastic coordinates $\mathbf{R}_{\text{slow}}$.

This is a general scheme, which can allow for additional considerations and further approximations. First, the average with respect to picoseconds dynamic processes is carried on, in practice, together with the average with respect to solvent coordinates to allow the QM evaluation of magnetic tensors corrected for solvent effects. Second, time-separation techniques can also be applied to treat approximately relatively faster relaxing coordinates included in the relevant set $\mathbf{R}_{\text{slow}}$, such as restricted (local) torsional motions. Third, complex solvent environments, such as for example highly viscous fluids, can be described by an augmented set of stochastic coordinates, to be included in $\mathbf{R}_{\text{slow}}$, which describes slow relaxing local solvent structures.[19]

In the case of MTPNN, we adopt the following hypotheses. We neglect explicit coupling with nuclei other than ^{14}N, and we consider a planar geometry for the molecule. This is equivalent, in many cases, to renouncing accurate description of any superhyperfine structure or inhomogeneous broadening in the spectra resulting from coupling with hydrogen nuclei. Estimates of inhomogeneous broadening line widths can be obtained from calculated values of $\mathbf{A}_n$ tensors.

Although at least two relevant internal degrees of freedom (i.e. dihedral angles) can be identified between the CH_3S- group and the phenyl ring and between the two rings, the former motion affects very slightly the magnetic parameters, and therefore it can be neglected, whereas we may assume that the second angle is affected by localized librations around the planar conformation (see next section). To simplify our methodology we shall not consider explicitly the coupling with this relatively soft degree of freedom which will be addressed elsewhere.[24]

(24) Barone V.; Polimeno, A. Manuscript in preparation.

The final set of stochastic relevant coordinates is therefore restricted to the set of orientational coordinates $\mathbf{R}_{slow} \equiv \Omega$; these are described in terms of a simple formulation for a diffusive rotator, characterized by a diffusion tensor **D**. The diffusion tensor is determined by the shape of the molecule, deriving from the minimum energy conformations obtained from the QM calculations. Our choice is formalized by adopting the following simple form for $\hat{\Gamma}$[24]

$$\hat{\Gamma} = \hat{J}(\Omega)\cdot\mathbf{D}\cdot\hat{J}(\Omega) \qquad (6)$$

where $\hat{J}(\Omega)$ is the angular momentum operator for body rotation.[25] The Boltzmann distribution (equilibrium solution) is simply $P_{eq} = 1/8\pi^2$. By defining $\hat{J}(\Omega)$ and **D** in the MF, a convenient form of eq 6 is obtained which is directly written in terms of the diffusion tensor principal values.

We can summarize the ICA applied to MTPNN as follows. Modeling based on the SLE approach requires the characterization of magnetic parameters (e.g. hyperfine for ^{14}N nuclei and Zeeman tensors). Integration among (1) evaluation of magnetic tensor parameters via QM calculation, with corrections based on averaging of fast motions, (2) explicit modeling of slow motional processes via stochastic treatment, and (3) evaluation of ESR spectra via SLE is the basic strategy behind a sound ab initio approach to interpretation of ESR data. Notice that shape-dependent dissipative parameters (e.g., rotational diffusion tensor) included in stochastic models can be obtained via a simple but effective hydrodynamic model.

Once the effective Liouvillean is defined, the direct calculation of the cw-ESR signal is possible without resorting to a complete solution of the SLE. Rather one can evaluate the spectral density from the expression[14,19]

$$I(\omega - \omega_0) = \frac{1}{\pi}\{Re\}\langle v|[i(\omega - \omega_0) + i\hat{L}]^{-1}|vP_{eq}\rangle \qquad (7)$$

where the Liouvillean $\hat{L}$ acts on a starting vector which is defined as proportional to the x component of the electron spin operator $\hat{S}_x$: in the present case one has

$$|vP_{eq}^{1/2}\rangle = [I_1 I_2]^{-1/2}|\hat{S}_x \otimes 1_1 \otimes 1_2 P_{eq}^{1/2}\rangle$$

where $I_1 = I_2 = 1$; here P_{eq} is the Boltzmann distribution in Ω-space, ω is the sweep frequency, and $\omega_0 = g_0\beta_e B_0/\hbar = \gamma_e B_0$, where $g_0 = T_r(\mathbf{g})/3$. Basic parameters for the direct evaluation of eq 7 are therefore the following: principal values and orientation of hyperfine tensor for the two ^{14}N nuclei $\mathbf{A}_1$ and $\mathbf{A}_2$, principal values and orientation of Zeeman tensor **g**, and finally the knowledge of the rotational diffusion tensor **D** is required, for the specific solvent (toluene).

The system geometry is summarized in Figure 2. A set of Euler angles Ω defines the relative orientation of a molecular frame (MF), fixed rigidly on the nitroxide ring, with respect to the LF; the local magnetic frames are in turn defined with respect to MF by proper sets of Euler angles.

III.C. Evaluation of Structural Parameters and Magnetic Tensors. The **g** tensor can be dissected into three main contributions:[6–9]

$$\mathbf{g} = g_e\mathbf{1}_3 + \Delta g^{RMC} + \Delta g^{GC} + \Delta g^{OZ/SOC} \qquad (8)$$

where g_e is the free electron value ($g_e = 2.002319$) and $\mathbf{1}_3$ is the 3 × 3 unit matrix. Δg^{RMC} and Δg^{GC} are first-order contributions, which take into account relativistic mass (RMC) and gauge (GC) corrections, respectively. The last term, $\Delta g^{OZ/SOC}$, is a second-order contribution arising from the coupling of the orbital Zeeman (OZ) and the spin−orbit coupling (SOC) operators. The SOC term is a true two-electron operator, but here it will be approximated by a one-electron operator involving adjusted effective nuclear charges.[26] This approximation has been proven to work fairly well in the case of light atoms, providing results close to those obtained using more refined expressions for the SOC operator.[6] In our general procedure, spin-unrestricted calculations provide the zero-order Kohn−Sham (KS) orbitals, and the magnetic field dependence is taken into account using the coupled perturbed KS formalism described by Neese, but including the GIAO approach.[6] Solution of the coupled perturbed KS equation (CP-KS) leads to the determination of the OZ/SOC contribution.

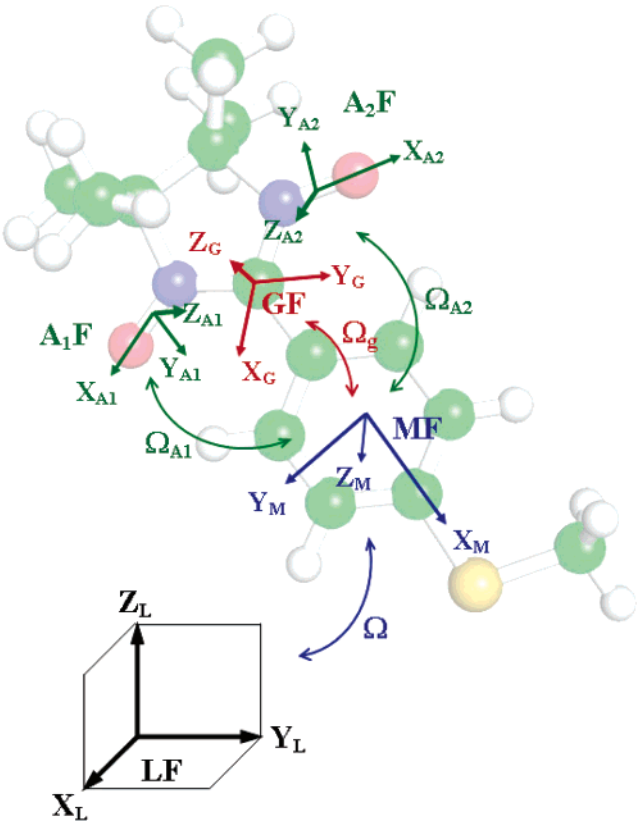

Figure 2. Reference frames employed in the stochastic Liouville equation.

The second term is the hyperfine interaction contribution which, in turn, contains the so-called Fermi-contact interaction (an isotropic term), which is related to the spin density at the corresponding nucleus n by[27]

$$A_{n,0} = \frac{8\pi}{3}\frac{g_e}{g_0}g_n\beta_n\sum_{\mu,\nu}P_{\mu,\nu}^{\alpha-\beta}\langle\varphi_\mu|\delta(r_{kn})|\varphi_\nu\rangle \qquad (9)$$

and an anisotropic contribution, which can be derived from the

(25) (a) Favro, L. D. *Phys. Rev.* **1960**, *119*, 53. (b) P. S. Hubbard *Phys. Rev.* **1972**, *A6*, 2421. (c) Fixman, M.; Rider, K. *J. Chem. Phys.* **1969**, *51*, 2429.
(26) Koseki, S.; Schmidt, M. W.; Gordon, M. S. *J. Phys. Chem.* **1992**, *96*, 10768.
(27) Fermi, E. *Z. Phys.* **1930**, *60*, 320.

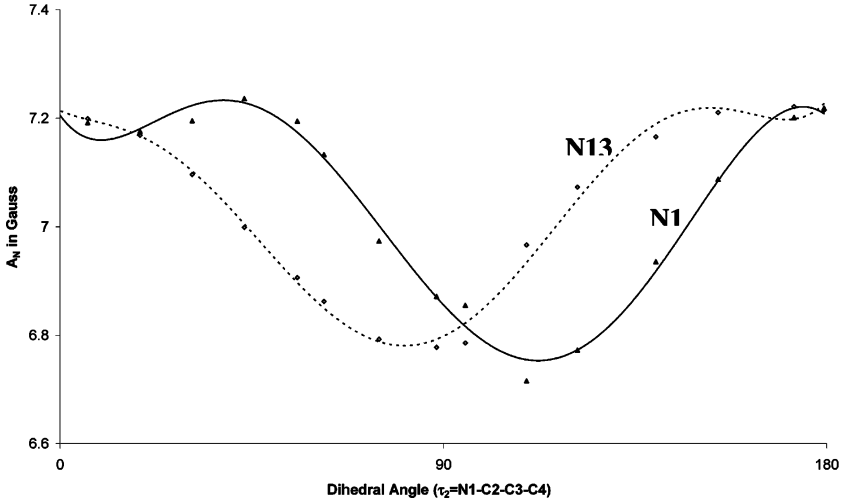

Figure 3. Dependence of the two nitrogen (N1 and N13) isotropic hyperfine coupling constants on the τ dihedral angle.

classical expression of interacting dipoles[28]

$$A_{n,ij} = \frac{g_e}{g_0} g_n \beta_n \sum_{\mu,\nu} P_{\mu,\nu}^{\alpha-\beta} \langle \varphi_\mu | r_{kn}^{-5} (r_{kn}^2 \delta_{i,j} - 3 r_{kn,i} r_{kn,j}) | \varphi_\nu \rangle \tag{10}$$

A tensor components are usually given in gauss (1 G = 0.1 mT); to convert data to MHz one has to multiply by 2.8025.

All the computations have been performed by the G03 package[29] using the parameter-free PBE0 functional[30] and the 6-31+G(d,p) basis set.[31] Solvent effects on energies and magnetic tensors have been evaluated by the latest implementation of the so-called polarizable continuum model (PCM).[32] This computational approach has been validated in a number of studies of magnetic properties of free radicals in non-protic solvents.[33]

A full geometry optimization of MTPNN in the gas phase leads to a nearly planar arrangement in which all the structural parameters are close to those reported in a previous study for related nitronylnitroxides,[34] except for a slight nonplanarity of the nitronylnitroxide ring, related to the steric hindrance of the four methyl groups. Since the general agreement with available experimental data[17] is satisfactory and no unexpected trends are found, we do not discuss structural aspects in detail. Then, a relaxed scan around the C7−C8−S18−C19 dihedral angle (Figure 1) results in a quite small energy barrier for the perpendicular orientation of the ring and the methyl group (about 2 kcal/mol in gas phase). In any case, the dependence of magnetic tensors on this dihedral angle is completely negligible. The situation is more involved for the N1−C2−C3−C4 dihedral angle (hereafter τ), which has an energy minimum for $\tau \approx 0°$ and a significant barrier for $\tau \approx 90°$ (about 7 and 5 kcal/mol in gas-phase and toluene, respectively). At the same time, the magnetic tensors show a significant dependence on this dihedral angle. For purposes of illustration the trends of the isotropic part of the hyperfine tensor and the g_{xx} component are shown in Figures 3 and 4, respectively. It is noteworthy that the variation of **g** is dominated by its g_{xx} component directed along the NO bond.

In view of the very low polarity of toluene we expect quite small solvent effects for both **g** and hyperfine tensors, and this expectation is confirmed by explicit PCM computations, which lead to differences between gas phase and toluene solution never exceeding 0.00004 ppm and 0.10 G for **g** and hyperfine tensors, respectively. It seems, therefore, quite justified to use, in the following dynamical treatment, averaged values of magnetic tensors computed in the gas phase, i.e. $g_{xx} = 2.00683$, $g_{yy} = 2.01142$, $g_{zz} = 2.00226$ and $A_{1,xx} = A_{2,xx} = 18.2$, $A_{1,yy} = A_{2,yy} = 1.997$, $A_{1,zz} = A_{2,zz} = 1.743$. Euler angles, specifying the relative orientation of magnetic tensors with respect to the molecular frame MF, which is chosen by definition as the molecule-fixed frame, which diagonalize the rotational diffusion tensor are given in the next section.

III.D. Evaluation of Rotation Diffusion Tensor. Let us briefly summarize the overall procedure, in its simplest implementation, to estimate diffusion properties of molecular systems, with internal degrees of freedom, based on a hydrodynamic approach.[35] We may start from a simplified view of the molecule under investigation as an ensemble of N fragments, each formed by spheres representing atoms or groups of atoms, immersed in a homogeneous isotropic fluid of known viscosity. Let us assume that the ith fragment is composed by N_i spheres (extended atoms) and that the torsional angle ϑ_i defines the relative orientation of fragments i and $i+1$. We denote by $\mathbf{u}_i$ the unitary vector for the corresponding bond. A total of $N - 1$ torsional angles/bonds are present, and each fragment has n_i atoms. For convenience, each $\mathbf{u}_i$ points from an atom in fragment i to an atom in fragment $i+1$ for $i \geq \nu$ and points from an atom in fragment $i+1$ to an atom in fragment i for $i < \nu$.

(28) Frosch, R. A.; Foley, H. M. *Phys. Rev.* **1952**, *88*, 1337.
(29) Frisch, M. J.; et al. *Gaussian03*, Revision C.02; Gaussian, Inc.: Pittsburgh, PA, 2003.
(30) Adamo, C.; Barone, V. *J. Chem. Phys.*. **1999**, *10*, 6158.
(31) Franci, M. M.; Petro, W. J.; Hehre, W. J.; Binkley, J. S.; Gordon, M.-H.; DeFree, D. J.; Pople, J. A. *J. Chem. Phys.* **1982**, *77*, 3654.
(32) (a) Cossi, M.; Scalmani, G.; Rega, N.; Barone, V. *J. Chem. Phys*. **2002**, *117*, 43. (b) Scalmani, G.; Barone, V.; Kudin, K. N.; Pomelli, C. S.; Scuseria, G. E.; Frisch, M. J. *Theor. Chem. Acc*. **2004**, *111*, 90. (c) Tomasi, J.; Mennucci, B.; Cammi, R. *Chem. Rev.* **2005**, *105*, 2999.
(33) (a) Barone, V. *Chem. Phys. Lett*. **1996**, *262*, 201. (b) Rega, N.; Cossi, M.; Barone, V. *J. Chem. Phys.* **1996**, *105*, 11060. (c) Tedeschi, A. M.; D'Errico, G.; Busi, E.; Basosi, R.; Barone, V. *Phys. Chem. Chem. Phys*. **2002**, *4*, 2180.
(34) (a) di Matteo A.; Adamo, C.; Cossi, M.; Rey, P.; Barone, V. *Chem. Phys. Lett*. **1999**, *310*, 159. (b) Adamo, C.; di Matteo, A.; Rey, P.; Barone, V. *J. Phys. Chem. A* **1999**, *103*, 3481.
(35) (a) Moro, G. *Chem. Phys*. **1987**, *118*, 167. (b) Moro, G. *Chem. Phys.* **1987**, *118*, 181.

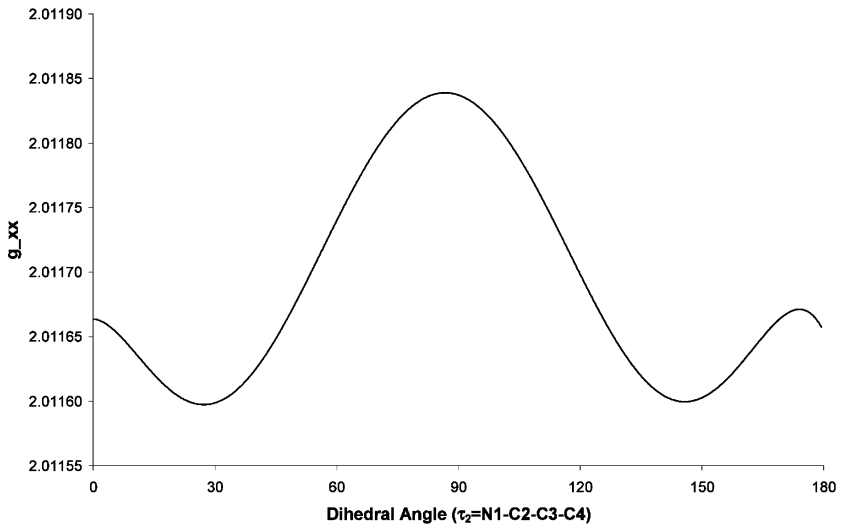

Figure 4. Dependence of the g_{xx} component on the τ dihedral angle.

Notice that the definition of the MF in a flexible system is somewhat arbitrary, and can be essentially left to convenience arguments. For sake of simplicity we may assume that MF is fixed on generic fragment ν.

By definition, in the MF, atoms of fragment ν have only translational and rotational motions, whereas atoms of all other fragments have additional internal rotational motions. Let us now associate the set of coordinates ($\mathbf{R}$, Ω, ϑ), which describe the translational, rotational, and internal torsional motions respectively, with the generalized velocities $\mathbf{V} \equiv (\mathbf{W},\omega,\vartheta)$ including the molecule translational velocity, angular velocity around an inertial frame, and associated torsional momenta. In the presence of constraints in and among fragments, the generalized force $\mathbf{F}$, made of force $\mathbf{\Phi}$, torque $\mathbf{N}$, and the internal torques $\mathbf{N}^{\text{int}}$, is related to the generalized velocities through the friction tensor Ξ, via the relation $\mathbf{F} = -\Xi\mathbf{V}$, while in the absence of constraints a similar relation hold for each single extended atom between its velocity and the force acting on it, $\mathbf{f}_j^i = -\xi\mathbf{v}_j^i$, where $\mathbf{f}_j^i$ is the force acting on jth atom of ith fragment ($1 \le j \le n_i$) etc. Constrained and unconstrained forces and velocities can be related via geometric considerations by the relations $\mathbf{F} = \mathbf{Af}$ and $\mathbf{V} = \mathbf{Bv}$, where $\mathbf{A}$ and $\mathbf{B}$ are matrices depending on the molecular geometry and one can show easily by inspection that $\mathbf{A} = \mathbf{B}^{tr}$. It follows that $\Xi = \mathbf{B}^{tr}\xi\mathbf{B}$. For a system of linearly connected fragments it is relatively simple to evaluate matrix $\mathbf{B}$ as a function of atomic positions $\mathbf{r}_j^i$.

By assuming now a form for the friction tensor of nonconstrained atoms, ξ, one can calculate the friction for the constrained atoms, Ξ. We may assume for simplicity the simplest model for noninteracting spheres in a fluid, namely that matrix ξ has only diagonal blocks of the form $\xi(T)\mathbf{1}_3$ where $\xi(T)$ is the translational friction of a sphere of radius R_0 at temperature T and given by the Stokes law $\xi(T) = CR\eta(T)\pi$, where $\eta(T)$ is the solvent viscosity at the given temperature T and C depends on hydrodynamic boundary conditions. The system friction is then given as $\Xi = \xi(T)\mathbf{B}^{tr}\mathbf{B}$. The diffusion tensor (which can be conveniently partitioned in translation, rotational, internal and mixed blocks) can now be obtained as the inverse of the friction tensor[35]

$$\mathbf{D} = \begin{pmatrix} \mathbf{D}_{TT} & \mathbf{D}_{TR} & \mathbf{D}_{TI} \\ \mathbf{D}_{TR}^{tr} & \mathbf{D}_{RR} & \mathbf{D}_{RI} \\ \mathbf{D}_{TI}^{tr} & \mathbf{D}_{RI}^{tr} & \mathbf{D}_{II} \end{pmatrix} = k_{\text{B}} T\, \Xi^{-1} \tag{11}$$

and neglecting off-diagonal couplings, an estimate of the rotational diffusion tensor is given by $\mathbf{D}_{RR} \equiv \mathbf{D}$, which depends directly on the atomic coordinates, temperature, and the solvent viscosity.

In the case of MTPNN dependence of the molecular geometry upon two relevant torsional angles does not affect substantially the overall steric hindrance (cf. Figure 5). Therefore, dependence of $\mathbf{D}$ upon torsional angles is neglected altogether.

Assuming a completely planar geometry, we can write the diffusional tensor (already diagonalized in the MF) in the form $\mathbf{D}(T) = \mathbf{D}(T)\mathbf{d}$ where $D(T) = k_{\text{B}}T/\xi(T)$ is the translational diffusional coefficient of a sphere or radius R at temperature T and $\mathbf{d}$ is a diagonal tensor depending only on the molecular geometry, with values $d_{xx} = 0.1795 \times 10^{18}$, $d_{yy} = 0.2238 \times 10^{18}$, and $d_{zz} = 1.072 \times 10^{18}$ m^{-2}.

Absolute determination of the rotational diffusion tensor is difficult within the limitations of the present coarse-grained approach, which describes the molecules as macroscopic objects immersed in a continuous fluid. Rather, it is convenient to refer the temperature dependence to a standard state by defining

$$D(T) = D(T_0)\cdot\frac{\eta(T_0)}{\eta(T)}\cdot\frac{T}{T_0}$$

where

$$D(T_0) = \frac{k_{\text{B}}}{RC\pi}\cdot\frac{T_0}{\eta(T_0)}$$

is the translational diffusion coefficient for a sphere of radius R at reference temperature T_0. The number $D(T_0)$ can be chosen once for all as an adjustable parameter. Taking as reference temperature $T_0 = 292$ K for which $\eta(T_0) = 595$ μPa s,[36] the

(36) Assael, M. J.; Dalaouti, N. K.; Dymond, J. H. *Int. J. Thermophys.* **2000**, *21*, 291. (b) Barlow, A. J.; Lamb, J.; Matheson, A. J. *Proc. R. Soc. London, Ser. A* **1966**, *292*, 322.

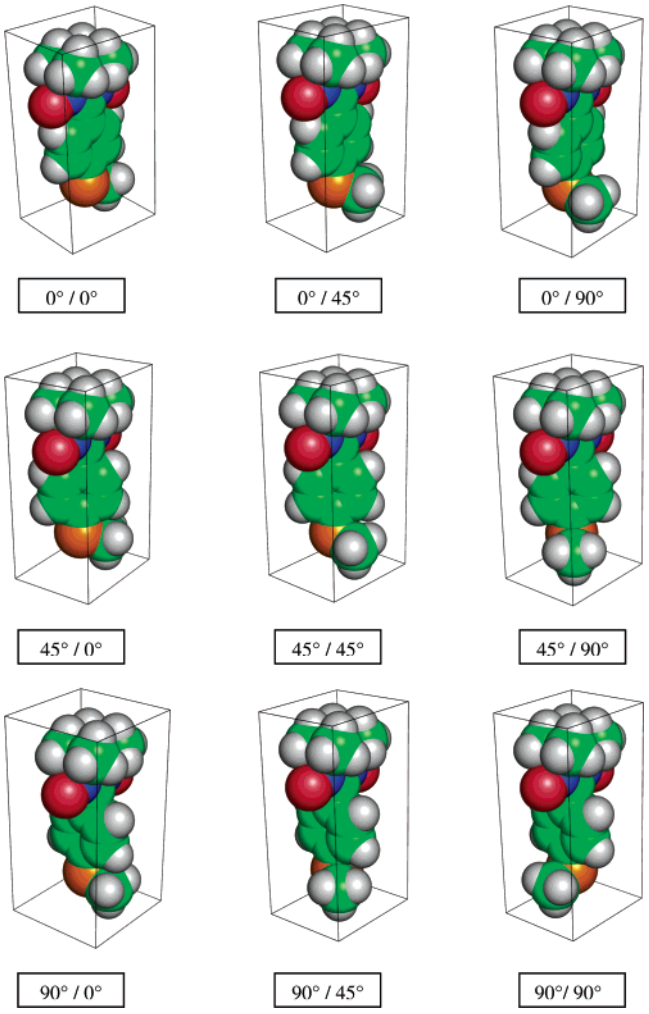

Figure 5. Sterical hindrance of MTPNN upon variation of torsional angles.

best agreement (see below) with experimental data has been achieved by choosing $D(T_0) = 1.498 \times 10^{-8}$ m^2 s^{-1}.

The relative orientation of the magnetic frames GF, A_iF can now be given explicitly, in terms of sets of Euler angles; the relative orientation of GF with respect to MF is given by $\Omega_g = (0°,45°,89°)$ while A_1F and A_2F are rotations of $\Omega_{A1} = (17°, -84°, 81°)$ and $\Omega_{A2} = (-164°, -81°, 66°)$, respectively. A slightly asymmetric disposition of A_1F and A_2F is due to molecular distortion of the minimized conformation from perfectly planar geometry and averaging.

III.E. Computational Evaluation of SLE. Once the magnetic and dissipative parameters are known, the numerical evaluation of eq 7 is carried out, adopting standard techniques. The computational implementation has been presented in detail elsewhere.[19] It is essentially based on a standard linear algebraic formulation of the resolvent in terms of matrices/vectors by projecting the Liouvillean $\hat{L}$ and the starting vector $|v\rangle$ on a suitable basis set that in our case can be initially defined as the direct product of spin operators of the two nuclei and the unpaired electron and of normalized Wigner rotation matrices which correspond to the rotational degrees of freedom. Matrix elements of the stochastic Liouvillean are determined algebraically, employing symmetry arguments to reduce the matrix dimension exactly. Approximate techniques, based on pruning schemes of the complete basis set, can also be employed.[14]

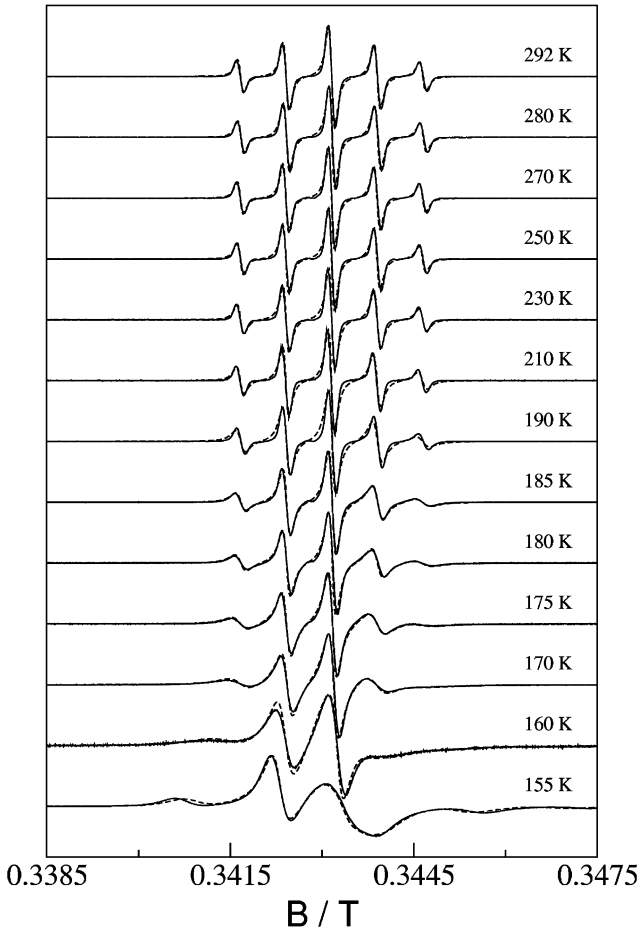

Figure 6. Experimental (full line) and simulated (dashed line) cw-ESR spectra of MTPNN in toluene in the temperature range 155−292 K.

Finally, eq 7 can be converted in matrix/vector form, and standard algorithms for tridiagonalization and direct evaluation of spectral densities in continuous fraction form can be employed, such as Lanczos or conjugate gradient.[14]

IV. Results and Discussion

The series of experimental spectra are compared with the outcomes of eq 4. Magnetic and diffusion tensors principal values and orientation have been taken from QM calculations, according to the computational approaches described in the previous sections. The only adjustable parameters, valid for the entire set of spectra, are the reference translational diffusion coefficient, $D(T_0) = 1.498 \times 10^{-8}$ m^2 s^{-1}, and an inhomogeneous broadening constant which has been taken equal to 4.7 G for $T > 190$ K, 2.8 G for 190 K $< T <$ 170 K, and 0 G for $T < 170$ K. Inhomogeneous broadening is required in order to account for residual line width resulting from superhyperfine coupling with hydrogen nuclei, which are not accounted for explicitly in the simplified Hamiltonian defined in eq 5. Notice that it is feasible (*i*) on the basis of the evaluation of coupling constants resulting from the QM calculation, to estimate A coupling terms for all hydrogen atoms and (*ii*) via a partial averaging of an extended SLE which include super-hyperfine coupling to evaluate the inhomogeneous broadening constant and its weak temperature dependence.[24]

The spectra are then calculated without further adjustments of temperature-dependent fitted parameters. In Figure 6, we

Table 1. Measured Values of g_0^{exp} for Four Temperatures

T/K	g_0^{exp}	estimated error
292	2.00681	±0.0001
280	2.00727	±0.0002
230	2.00695	±0.0002
210	2.00720	±0.0002

compare the experimental (full line) and simulated (dashed line) cw-ESR spectra of MTPNN in toluene in the temperature range 155−292 K. Since experimental spectra at different temperatures have been measured at slightly varying frequencies, ν_0, in Figure 6 spectra are reported relative to their respective central field, B_0, for the reader's convenience, i.e., implementing eq 7 as such. Notice however that no adjustment is required in the absolute position of the spectra. In fact the measured value of g_0 at room temperature ($g_0 = 2.00681$) matches perfectly the predicted theoretical value, obtained as one-third of the trace of the **g** tensor, $g_0^{calc} = 2.00686$. On the other hand the measured g_0 values are independent of the temperature inside the experimental error, see Table 1.

On the other side, the overall very satisfactory agreement of the spectra band-shape, particularly at low temperatures, is a convincing proof that the simplified dynamic modeling implemented in the SLE through the purely rotational stochastic diffusive operator $\hat{\Gamma}$, eq 6, and the hydrodynamic calculation of the rotational diffusion tensor, section II.C, is sufficient to describe the main slow relaxation processes. In our opinion, the above results show the potentialities of an integrated computational approach and the validity of the assumptions made in the specific application. In particular, the complete Hamiltonian of a radical interacting with the solvent molecules has been reduced by means of a series of approximations based on separations of motions taking advantage of their different time scale. In the first main step of the calculation, by a QM treatment the spin Hamiltonian of the paramagnetic probe is extracted, with magnetic parameters averaged on the electron and fast vibrational nuclear motions, and corrected for solvent effects. The minimum energy conformations of the molecule are evaluated. In the second step, the motions in solution are then approached by a classical mechanical treatment within the framework of the stochastic Liouville equation. A stochastic operator $\hat{\Gamma}$ is built up in terms of the diffusion tensor principal values, based on the previously calculated molecular geometry and solvent thermodynamic properties. The spectral profile is then obtained by numerical integration of the Liouville equation.

The excellent agreement between calculated and experimental spectra shows that the ICA can start a new page in the field of ESR spectra interpretation. This procedure has been applied here to a radical in a single phase, but with magnetic interactions more complex than those typical of a nitroxide spin probe. The success of this method when applied to more challenging systems can be foreseen, as it is based on the link between (1) sophisticated QM calculations of molecular properties giving amazingly reliable magnetic parameters tailored for each environment of the probes and (2) refined stochastic models for their reorientational motions in any dynamical régime and orienting potential symmetry.

As in the applications to complex systems (biological systems, composite materials) one must take into account different phases embedding the radical or motions in different dynamical ranges or both; otherwise, the results obtained by the traditional simulation approach are doomed to a substantial ambiguity, as the number of adjustable parameters increases beyond the limit of a trustable unique set. On the other hand in the ICA, a self-consistent model for each molecular environment of the radical is used, where all the relevant parameters are entangled and no one can be changed independently. The higher reliability of this approach is evident.

Acknowledgment. This work was supported by the Italian Ministry for University and Research, projects FIRB, PRIN ex-40%, and the National Institute for Materials Science and Technology, project PRISMA 2005.

Supporting Information Available: Complete ref 29. This material is available free of charge via the Internet at http://pubs.acs.org.

JA065475Q